Differences in frontal network anatomy across primate species

Barrett, Rachel L.C.; Dawson, Matthew; Dyrby, Tim B.; Krug, Kristine; Ptito, Maurice; D'Arceuil, Helen; Croxson, Paula L.; Johnson, Philippa J.; Howells, Henrietta; Forkel, Stephanie J.

Total number of authors:
12

Published in:
Journal of neuroscience

Link to article, DOI:
10.1523/JNEUROSCI.1650-18.2019

Publication date:
2020

Document Version
Peer reviewed version

JNeurosci
THE JOURNAL OF NEUROSCIENCE

Research Articles: Systems/Circuits

Differences in frontal network anatomy across primate species

https://doi.org/10.1523/JNEUROSCI.1650-18.2019

Cite as: J. Neurosci 2020; 10.1523/JNEUROSCI.1650-18.2019

Received: 27 June 2018
Revised: 14 November 2019
Accepted: 15 November 2019

Differences in frontal network anatomy across primate species

Rachel L. C. Barrett[a,b], Matthew Dawson[b], Tim B. Dyrby[c,d], Kristine Krug[e,f,g], Maurice Ptito[h,i], Helen D'Arceuil[j], Paula L. Croxson[k], Philippa Johnson[a,l], Henrietta Howells[a,b,m], Stephanie J. Forkel[a,b], Flavio Dell'Acqua[a,b,1], and Marco Catani[a,b,1]

[a]NatBrainLab, Department of Neuroimaging, Institute of Psychiatry, Psychology and Neuroscience, King's College London, London, SE5 8AF, UK; [b]NatBrainLab, Sackler Institute for Translational Neurodevelopment, Department of Forensic and Neurodevelopmental Science, Institute of Psychiatry, Psychology and Neuroscience, King's College London, London, SE5 8AF, UK; [c]Danish Research Centre for Magnetic Resonance, Centre for Functional and Diagnostic Imaging and Research, Copenhagen University Hospital Hvidovre, Hvidovre, DK-2650, Denmark; [d]Department of Applied Mathematics and Computer Science, Technical University of Denmark, Kongens Lyngby, DK-2800, Denmark; [e]Department of Physiology, Anatomy and Genetics, University of Oxford, Oxford, OX1 3PT, UK; [f]Institute of Biology, Otto-von-Guericke-Universität Magdeburg, 39120, Germany; [g]Leibniz-Institute for Neurobiology, Magdeburg, 39118, Germany; [h]Laboratory of Neuropsychiatry, Psychiatric Centre Copenhagen, Copenhagen, DK-2200, Denmark; [i]École d'Optométrie, Université de Montréal, Montréal, Québec, H3T 1P1, Canada; [j]Athinoula A . Martinos Center for Biomedical Imaging, Massachusetts General Hospital, Charlestown, Massachusetts, 02129, USA; [k]Department of Neuroscience and Friedman Brain Institute, Icahn School of Medicine at Mount Sinai, New York, New York, 10029. USA; [l]College of Veterinary Medicine, Cornell University, Ithaca, New York, 14853, USA; [m]Laboratory of Motor Control, Department of Medical Biotechnologies and Translational Medicine, Università degli Studi di Milano, Humanitas Research Hospital, IRCCS, Milan, 20129, Italy.

[1]F.D'A. (Flavio Dell'Acqua) and M.C. (Marco Catani) contributed equally to this work.

Correspondence should be addressed to:
Marco Catani
Institute of Psychiatry, Psychology and Neuroscience
King's College London
16 De Crespigny Park
London, SE5 8AF, UK
Email: m.catani@iop.kcl.ac.uk

Number of pages 25

Number of figures: 7 figures, 6 tables

Number of words: Abstract 227 Significance Statement 115, Introduction 612, and Discussion 1500

Author contributions: M.C. and R.B. designed the experiment. T.D. and H.D'A. developed the *ex vivo* imaging protocols. M.P. and T.D. supplied the vervet *ex vivo* datasets, K.K. and T.D. supplied the *ex vivo* rhesus macaque datasets, and H. D'A. supplied the *ex vivo* cynomolgus macaque datasets. P.C. supplied the *in vivo* rhesus macaque datasets. F.D'A. developed acquisition protocols for the human datasets and developed the tractography-processing pipeline. H.H. and F.D'A collected the in-vivo human data. R.B. and F.D'A. processed the tractography data. R.B, M.D. and P.J. dissected the tractography data under M.C.'s guidance. R.B performed the voxel-based and tractography volume analyses and statistical analysis. M.C. and R.B. prepared the figures. M.C., R.B., M.D., H.H. and S.F. contributed to writing the manuscript, which was edited by all authors.

Conflict of Interest: The authors declare no competing financial interests.

Acknowledgements: We thank Lazar Fleysher, Rafael O'Halloran, Hauke Kolster, Christienne Damatac, Jamie Nagy, Ronald Primm, Pedro Hernandez and Ignacio Medel for help in acquiring the *in vivo* macaque datasets, and Leonardo Cerliani for assistance with cynamolgus macaque datasets. We are grateful to members of the NatBrainLab and Department of Forensics and Neurodevelopmental Sciences, King's College London, for feedback and suggestions. This research was supported by the Wellcome Trust Investigator Award 103759/Z/14/Z to M.C. This paper represents independent research partly funded by the National Institute for Health Research (NIHR) Biomedical Research Centre at South London and Maudsley NHS Foundation Trust and King's College London. The views expressed are those of the author and not necessarily those of the NHS, the NIHR or the Department of Health.

Abstract

The frontal lobe is central to distinctive aspects of human cognition and behavior. Some comparative studies link this to a larger frontal cortex and even larger frontal white matter in humans compared with other primates, yet others dispute these findings. The discrepancies between studies could be explained by limitations of the methods used to quantify volume differences across species, especially when applied to white matter connections. In this study, we used a novel tractography approach to demonstrate that frontal lobe networks, extending within and beyond the frontal lobes, occupy 66% of total brain white matter in humans and 48% in three monkey species, *Chlorocebus aethiops, Macaca mulatta* and *Macaca fascicularis*, all male. The simian-human differences in proportional frontal tract volume were significant for projection, commissural and both intra- and interlobar association tracts. Among the long association tracts the greatest difference was found for tracts involved in motor planning, auditory memory, top-down control of sensory information, and visuospatial attention, with no significant differences in frontal limbic tracts important for emotional processing. In addition we found that a non-frontal tract, the anterior commissure, had a smaller volume fraction in humans, suggesting that the disproportionally large volume of human frontal lobe connections is accompanied by a reduction in the proportion of some non-frontal connections. These findings support a hypothesis of an overall rearrangement of brain connections during human evolution.

Significance Statement

Tractography is a unique tool to map white matter connections in the brains of different species including humans. This study shows that humans have a greater proportion of frontal lobe connections compared with monkeys, when normalized by total brain white matter volume. In particular, tracts associated with language and higher cognitive functions are disproportionally larger in humans compared with monkeys, whereas other tracts associated with emotional processing were either the same or disproportionally smaller. This supports the hypothesis that the emergence of higher cognitive functions in humans is associated with increased extended frontal connectivity, allowing human brains more efficient cross-talk between frontal and other high order associative areas of the temporal, parietal and occipital lobe.

Introduction

The frontal lobe is considered to play an important role in high level cognitive functions with differences across species (Passingham and Wise, 2012), and is relatively large in humans compared with other vertebrates (Fuster, 1988). When humans are compared with higher primates, however, the results are mixed, with some reporting no difference in the proportion of frontal (Semendeferi et al., 2002) or prefrontal (Schoenemann et al., 2005) cortical volume. This turned more attention to white matter in line with Zhang and Sejnowsky (2000), who proposed that longer white matter fibers are required by larger brains to guarantee efficient communication between distant cortical areas. Smaers et al. (2011; 2017) and Donahue et al. (2018) reported that the prefrontal cortex and white matter were disproportionally greater in humans than higher primates, yet others dispute these findings (Barton and Venditti, 2013; Gabi et al., 2016). This discrepancy in results could be explained by the lack of consensus on anatomical boundary delineation and the limitations of methods adopted (Sherwood and Smaers, 2013). Nonetheless there appears to be agreement in the literature that an expansion of distributed white matter networks, rather than cortical volume of the frontal lobe, may have had an important role in the evolution of human higher cognitive functions.

In this study we performed a comparative analysis of the white matter tracts of the frontal lobe using a novel approach based on diffusion tractography. Compared with structural magnetic resonance imaging (MRI) or tissue-sectioning methods that have previously been adopted to study the frontal lobe, tractography offers two main advantages. Firstly, tract volume can be approximated by calculating the space occupied by streamlines that follow the entire trajectory of white matter pathways. When applied to the frontal lobes, this allows us to analyze the large portion of frontal connections extending beyond the anatomical boundaries of the frontal lobe, which has not been taken into account with previous MRI approaches. Secondly, distinct tract groups and individual pathways can be virtually dissected and analyzed separately (Catani et al., 2002; Thiebaut de Schotten et al., 2012). Frontal lobe connections can be classified into three main tract groups that include projection fibers (linking the cortex with subcortical areas and the brain stem), commissural fibers (linking cortical areas between hemispheres) and association fibers (linking cortical areas within a single hemisphere). The latter can be further subdivided into

intralobar (within the frontal lobe) and interlobar (between frontal and non-frontal regions) connections (Catani et al., 2012b). Considering that various tracts and groups of tracts play distinct roles in cognition and behavior, a differentiated tract analysis between species may reveal differences in networks underlying uniquely human abilities (Passingham and Wise, 2012).

Diffusion imaging tractography was acquired from 20 human participants *in vivo*, nine non-human primates *ex vivo* (five macaques, four vervets) and six macaques *in vivo*. Diffusion data were analyzed using spherical deconvolution, an advanced diffusion modeling technique, which we have previously applied to reconstruct crossing fibers and visualize tracts that are not visible with tensor-based approaches (Dell'Acqua et al., 2010; Thiebaut de Schotten et al., 2011; Catani et al., 2012a; Dell'Acqua and Tournier, 2019). Deterministic tractography was used to calculate the total volume of frontal lobe white matter, frontal association, commissural and projection tract groups including long and short-range connections and finally, individual frontal lobe tracts. Additionally, a non-frontal tract, the anterior commissure was included in the analysis to verify that there may exist tracts in the brain that are disproportionally smaller in humans than monkeys. For each brain, frontal tract volume measurements were divided by total hemispheric tract volume to obtain normalized values. MRI voxel-based measurements of frontal cortical and white matter volume were also obtained for comparison with previous studies.

Materials and Methods

Participants. Diffusion MRI data were analyzed from 20 human *Homo sapiens* participants *in vivo* (all male, mean age ± standard deviation = 27.9 ± 5.0 years) and three monkey species *ex vivo*: four vervets (*Chlorocebus aethiops*, all male, age = 4.1 ± 1.9 years), three rhesus macaques (*Macaca mulatta*, all male, mean age 11.2 ± 2.0 years) and two cynomolgus macaques (*Macaca fascicularis*, all male, mean age estimated ≥ 11 years). In addition, six rhesus macaque (all male, mean age 5.5 ± 0.4 years) datasets were acquired *in vivo* for a comparison between *in vivo* and *ex vivo* tractography results. The human data were acquired with informed consent under the Biomedical Research Centre Atlas Project, approved by the Joint Medical Ethical Committee of the Institute of Psychiatry, Psychology and Neuroscience, King's College London.

The four vervet monkeys were obtained from the Behavioral Science Foundation, St. Kitts and were socially housed in enriched environments. The experimental protocol was reviewed and approved by the Institutional Review Board of the Behavioral Science Foundation acting under the auspices of the Canadian Council on Animal Care. The three rhesus macaque brains stem from a research program at the University of Oxford and all procedures were carried out in accordance with Home Office (UK) Regulations and European Union guidelines (EU directive 86/609/EEC; EU Directive 2010/63/EU) Act (1986). For details of tissue fixation, see Dyrby et al. (2011) and Large et al. (2016). The two cynomolgus macaque datasets were obtained from the Martinos Center for Biomedical Imaging. All housing, transport and experimental procedures were approved by the appropriate institutional animal care panels, described in de Crespigny et al. (2005) and the tissue was prepared as described in D'Arceuil et al. (2007).

The macaque *in vivo* datasets were obtained from the Icahn School of Medicine at Mount Sinai (ISMMS). The experimental procedures required for collecting this data were approved by the ISMMS Institutional Animal Care and Use Committee and conformed to the United States Public Health Service policy on Humane Care and Use of Laboratory Animals, the National Institutes of Health Guide for the Care and Use of Laboratory Animals and Association for Assessment and Accreditation of Laboratory Animal Care accreditation. They were socially housed as a group in an enriched environment. Scanning was carried out under light isoflurane anesthesia as described previously in Mars et al. (2011). Anesthesia was induced using ketamine (10 mg/kg intramuscularly) and maintained with isoflurane at a low concentration (0.9–1.7% expired; mean, 1.38%). Anesthesia was supplemented with meloxicam (0.2 mg/kg, intravenously, i.v.) and ranitidine (0.05 mg/kg, i.v.). Monkeys were intubated and ventilated throughout. Physiological parameters including capnography, inspired and expired isoflurane concentration, $SP0_2$, core temperature, heart rate and blood pressure were monitored and kept constant to maintain normal physiological function.

Diffusion MRI Acquisition. The human data were acquired on a 3T GE Signa HDx TwinSpeed MRI scanner using an echo planar imaging pulse sequence as described in Dell'Acqua et al. (2013). The vervet and rhesus macaque data were acquired with a 4.7T Varian Inova scanner using the protocol described by Dyrby et al. (2011); the cynomolgus macaque data were acquired with a 4.7T Oxford magnet

interfaced to a Bruker Biospec Avance console according to the parameters indicated by D'Arceuil et al. (2007). The *in vivo* rhesus macaque datasets were acquired with a Siemens Skyra 3T scanner with a custom-built 8-channel phased-array coil with a single loop local transmit coil (Windmiller-Kolster Scientific, Fresno, CA, USA). Spin echo pulse sequences were used to acquire the *ex vivo* monkey datasets, while the *in vivo* monkey datasets were acquired using an echo planar imaging sequence. The diffusion MRI acquisition parameters for all species are summarized in Table 1. The anatomical accuracy and reproducibility of post mortem diffusion MRI has previously been validated using axonal tracing (Dyrby et al., 2007; Jbabdi et al., 2013; Cerliani et al., 2016; Donahue et al., 2016).

Diffusion MRI and Tractography Processing. All steps from pre-processing to tractography tract dissections were performed in the native space of each individual brain. Data were inspected for artifacts visually and with the Explore DTI outlier profile tool. One volume in the cynomolgus macaque dataset was removed due to severe artefacts. The human diffusion data were corrected for head motion and eddy current distortions and registered to a non-diffusion-weighted reference image using ExploreDTI (www.exploredti.com). The *ex vivo* data did not undergo these corrections, as they were scanned using a spin echo sequence that is robust to eddy current and geometric distortions. For the *in vivo* macaque data, eight averages per brain were acquired, four with left-right phase-encoding direction and three with right-left, to facilitate correction for distortions along the phase encoding direction. After correction for susceptibility-induced off-resonance field effects using the tool Topup (Andersson et al., 2003) as implemented in FSL, datasets were registered and corrected for motion and eddy currents with FSL's Eddy (Andersson and Sotiropoulos, 2016).

For all datasets, the fiber orientation distribution function was estimated with StarTrack (www.natbrainlab.co.uk) using the damped Richardson-Lucy algorithm for spherical deconvolution as described in Dell'Acqua et al. (2010). Deterministic tractography was performed in each brain using the Euler algorithm in StarTrack (Dell'Acqua et al., 2013). A whole brain approach was used, with one seed point per voxel, and one streamline generated for each peak of the fiber orientation distribution function above the set anisotropy threshold. As the *ex vivo* data had varying levels of noise and voxel sizes, spherical deconvolution and tractography parameters were determined experimentally for each group in order to

maximize the ability to resolve crossing fibers, and minimize spurious fiber directions (see Table 2 for details). Anisotropic power maps (Dell'Acqua et al., 2014) were generated for anatomical reference, using StarTrack. The dissections were performed by R.B., M.D. and P.J. under the supervision of an expert anatomist (M.C.).

Tractography Analysis. The frontal white matter as a whole was dissected in TrackVis (www.trackvis.org) using an inclusion region of interest of the frontal lobe, as defined in humans by the standard MNI 152 nonlinear 6th generation MRI atlas segmentation (Collins et al., 1999) and in vervets and macaques, by the INIA19 MRI atlas (Rohlfing et al., 2012) (Fig. 1). These cortical atlas regions were co-registered to anisotropic power maps in the native space of each brain using Advanced Normalization Tools (ANTs, picsl.upenn.edu/software/ants). This was done separately for each hemisphere. To isolate the frontal association pathways, exclusion regions were drawn manually to remove any streamlines travelling to the opposite hemisphere (i.e. commissural connections), subcortical nuclei, cerebellum or brainstem (i.e. projections). Intra-frontal streamlines were defined similarly, but with the additional condition that both ends of the streamlines be within the frontal lobe region of interest. The frontal projection pathways were defined for each hemisphere using one inclusion region in the region of the basal ganglia and thalamus, including the internal capsule, and a second inclusion region of the frontal cortex. Frontal commissural pathways were defined to include all streamlines connecting the left and right frontal cortices and manually removing any streamlines not belonging to the corpus callosum. The cerebellar white matter and the volume of projection fibers below the level of the pons were excluded from the final volume analysis.

Manual dissections of individual frontal association tracts were performed. The tracts included in our analysis were the cingulum, uncinate fasciculus, frontal aslant tract, three branches of the superior longitudinal fasciculus, inferior fronto-occipital fasciculus and the long segment of the arcuate fasciculus. In addition, the anterior commissure was dissected as a non-frontal control tract. Tracts were dissected using manually drawn inclusion and exclusion regions of interest, as illustrated in Figure 2. Where multiple inclusion regions are needed to define a tract, a logical 'AND' condition was used, so that only streamlines passing through both regions were included in the result. The atlas by Catani and Thiebaut de Schotten (2012) was used as an anatomical reference for human tracts, and Schmahmann and Pandya's (2006)

axonal tracing atlas was used for the macaque and vervet datasets. For all dissections, large regions of interest extending into the white matter were used to ensure all relevant streamlines were captured and to avoid region-placement bias. The regions were then edited if necessary to remove irrelevant streamlines such as those identified as belonging to another tract, or with anatomically implausible trajectories such as looping. In tracts which are less well described, or less similar in the non-human species compared with humans, such as the frontal aslant tract and the arcuate fasciculus, atlas-defined rather than hand-drawn inclusion regions were used first to identify all streamlines projecting to the appropriate regions. The dissections were then refined using regions of interest in the white matter to capture only the streamlines from the given tract. Tractography volume measurements were obtained by calculating the total volume of voxels containing streamlines from the given tract. Normalized volumes were obtained by dividing the tract volume by the total volume occupied by hemispheric white matter streamlines, defined using a region of interest of the whole hemisphere, as shown in Figure 1.

Voxel-based Volume Analysis. Gray matter (excluding subcortical nuclei) and white matter (excluding cerebellar and white matter below the pons) tissue probability maps from the MNI (Fonov et al., 2009; 2011) and INIA19 (Rohlfing et al., 2012) templates were co-registered to anistropic power maps in the native space of each brain, using ANTS (Avants et al., 2011). A minimum probability threshold of 0.1 was applied and a weighted volume (i.e. volume × tissue probability value) was calculated, to obtain measures of gray and white matter volume that are robust to small errors in registration. The frontal volumes were calculated similarly, by first applying a frontal lobe mask to the tissue probability maps. To obtain normalized volume measures in each brain, frontal volume fractions were calculated as follows: the frontal cortex volume was divided by the total cortical volume and the frontal white matter volume divided by the total white matter volume. Absolute volumes were measured in milliliters (ml) and volume fractions calculated as percentages (%).

Experimental Design and Statistical Analysis. For statistical analysis the data were divided into three groups, humans (*in vivo*, n = 20), vervets (*ex vivo*, n = 4) and macaques (*ex vivo*, n = 5). The sample sizes in this study were determined by the availability of high quality *ex vivo* data in monkey species. Our statistical analysis was carried out on normalized volume measurements averaged across the two

hemispheres in each brain individually. To identify if there were species group differences within the different volume measures (voxel-based frontal white and cortical gray matter, tractography-based frontal white matter, frontal association, projection, commissural, and intra-frontal tract groups, and individual tracts), a one-way Welch ANOVA (Welch, 1951) using an asymptotically distributed F-statistic was applied with IBM SPSS version 20. In the measures with significant species group differences ($p < 0.05$), a Games-Howell *post hoc* analysis was applied to determine the specific differences between species groups (Games and Howell, 1976). Additionally, we compared the group of *in vivo* macaques ($n = 6$) with the *ex vivo* macaque and *in vivo* human data using Welch's F followed by Games-Howell *post hoc* tests, as above. The statistical tests used in this study were chosen for being robust to small group sizes and inhomogeneity of variance between groups (Games and Howell, 1976; Clinch and Keselman, 1982). Type I errors are controlled for by the Games-Howell *post hoc* analysis when carrying out multiple comparisons (Games and Howell, 1976). Results are reported as species group mean ± standard deviation. The data presented in this paper and the protocols and code used in the analysis will be available to readers upon request to the corresponding author.

Results

Figure 3 and Table 3 show the results for proportional and absolute volumes obtained with tractography and voxel-based MRI measurements of frontal cortical and white matter. The ANOVA of volume proportions indicated statistically significant differences among the three species groups for the frontal cortex (Welch's $F(2, 5.88) = 46.47$; $p < 0.001$), the voxel-based frontal white matter (Welch's $F(2, 5.65) = 1415.65$; $p < 0.001$) and the tractography-based frontal frontal white matter (Welch's $F(2, 5.60) = 84.03$; $p < 0.001$). Games-Howell *post hoc* analysis showed that human brains had a higher frontal cortex volume fraction (32.69 ± 0.79%) compared with both vervets (28.89 ± 0.79%; $p = 0.002$) and macaques (29.12 ± 1.22%; $p = 0.004$). The differences for the voxel-based frontal white matter volume fraction were even greater between humans (40.80 ± 0.62%) and both vervets (23.33 ± 0.72%; $p < 0.001$) and macaques (23.19 ± 1.04%; $p < 0.001$). Finally, our novel method using tractography to analyze the volume of frontal

lobe networks extending throughout the brain also showed a higher volume fraction in humans (66.18 ± 2.56%) compared with vervets (48.16 ± 2.94%; $p = 0.001$) and macaques (47.98 ± 4.54%; $p = 0.001$). No statistically significant differences existed between monkey species in these three measures (Table 3). These results confirm previous voxel-based findings (Schoenemann et al., 2005; Smaers et al., 2010) and indicate that our tractography measures are able to detect simian-human differences in tract volumes. The absolute frontal volume measurements were also significantly different between species, with humans greater than monkeys in all three measures. There were no statistically significant differences between monkey species in the absolute measurements of frontal gray matter volume ($F(2, 9.713) = 1122.75$, $p < 0.001$), voxel-based frontal white matter volume ($F(2, 10.48) = 1329.29$, $p < 0.001$) and tractography-based frontal white matter volume ($F(2, 13.53) = 632.49$, $p < 0.001$) (Table 3).

To examine the implication of humans having proportionally more frontal white matter than monkeys, we analyzed a non-frontal tract for comparison, the anterior commissure (Fig. 3. D; Table 3). The ANOVA of the volume fraction of the anterior commissure also indicated statistically significant differences among the groups (Welch's $F(2, 5.68) = 29.95$; $p = 0.001$) but in this case humans had a smaller volume fraction (4.59 ± 1.15%) compared with both vervets (9.90 ± 1.30%; $p = 0.004$ *post hoc*) and macaques (7.86 ± 1.80%; $p = 0.028$ *post hoc*). The volume fraction of the anterior commissure was not statistically significant different between the two monkey groups (Table 3). This suggests that the disproportionally large volume of frontal lobe tracts is accompanied by a reduced volume fraction of some non-frontal tracts, such as the anterior commissure. The absolute volume of this tract was significantly different between species, $F(2, 12.91) = 89.85$, $p < 0.001$), and was larger in humans than the two monkey species (Table 3).

To understand whether the larger volume proportion of frontal white matter in humans compared with monkeys was attributable to a specific tract group or a general trend across all frontal lobe connections, volume measurements of the association, projection and commissural tract groups were obtained separately and compared across species (Fig 4, Table 4). Statistically significant differences among the three groups were observed in the proportional frontal volume of the association (Welch's $F(2, 5.54) = 22.06$, $p = 0.002$), commissural (Welch's $F(2, 5.67) = 42.56$, $p < 0.001$) and projection (Welch's

F(2, 5.65) = 71.14, p < 0.001) tracts groups. *Post hoc* analysis shows that the frontal association tracts, which made up 36.69 ± 3.13% of the total white matter connection volume in humans, had a greater volume proportion compared with both vervets (25.92 ± 3.48%; p = 0.010) and macaques (23.15 ± 6.46%; p = 0.018). For the frontal commissural tracts, the volume fraction in humans (34.58 ± 3.30%) was higher than in vervets (27.85 ± 3.67%; p = 0.002) and macaques (26.19 ± 5.76%; p = 0.014). The projection tracts occupied 14.52 ± 1.44% of the total white matter volume in humans and only 4.80 ± 1.82% in vervets (p = 0.001) and 5.14 ± 2.25% in macaques (p = 0.001). In these three tract groups, no significant differences were found between the two monkey species. In addition, differences in proportional volume of the short intralobar association connections were detected (Welch's F(2, 9.52) = 113.33, p < 0.001) with humans showing higher values (16.33 ± 1.77%) compared with vervets (9.50 ± 0.73%; p < 0.001) and macaques (7.79 ± 1.04%; p < 0.001). Again no differences were found between the two monkey species. These results suggest that differences between humans and monkeys in the volume of the frontal lobe pathways are attributable to a global change in both interlobar (i.e. association, commissural and projections) and intralobar frontal connectivity. Absolute volumes of the above tract groups were also analyzed, revealing significantly larger volumes in humans, and no significant differences between monkey species (association tracts F(2, 10.95) = 535.787, p < 0.001; commissural tracts F(2, 13.54) = 338.48, p < 0.001; projection tracts F(2, 13.51) = 667.20, p < 0.001; intra-frontal tracts F(2, 13.61) = 376.22, p < 0.001 (Fig.4, Table 4).

We then investigated differences between species in the main long association tracts, which included the cingulum, uncinate fasciculus, frontal aslant tract, superior longitudinal fasciculus, inferior fronto-occipital fasciculus and the long segment of the arcuate fasciculus, using tractography dissections (Fig. 5, Table 5). There were no significant differences between species in the cingulum, with volume fractions of 4.06 ± 0.62% in humans, and 3.21 ± 0.29% in vervets and 3.04 ± 0.23 in macaques (F(2, 5.55) = 3.00, p = 0.131), the uncinate fasciculus, with 2.56 ± 0.69% in humans, 2.38 ± 0.39% in vervets and, 1.97 ± 0.53% in macaques (F(2, 6.51) = 0.731, p = 0.517), or the frontal aslant tract, with 3.37 ± 1.00% in humans, 2.35 ± 0.86% in vervets and 2.47 ± 0.92% in macaques (F(2, 6.68) = 3.01, p = 0.117). Significant differences in proportional volume were observed for all three branches of the superior longitudinal fasciculus. In humans, branches I, II and III occupied 3.46 ± 0.93%, 3.66 ± 1.17% and 3.65 ± 1.08% of the total hemispheric white matter volume respectively, in vervets, 0.71 ± 0.36%, 1.12 ± 0.36% and 1.33 ±

0.06%, and in macaques, 1.22 ± 0.44%, 1.06 ± 0.55% and 1.54 ± 1.02% (branch I, Welch's $F(2, 9.71) = 54.13$, $p < 0.001$; branch II, Welch's $F(2, 10.20) = 40.12$, $p < 0.001$; branch III, Welch's $F(2, 9.04) = 27.78$, $p < 0.001$). The inferior fronto-occipital fasciculus had volume proportions of 9.59 ± 1.22% in humans, 3.80 ± 0.89% in vervets and 3.25 ± 0.94% in macaques (Welch's $F(2, 7.30) = 101.22$, $p < 0.001$) and most strikingly the arcuate fasciculus had a proportional volume of 8.96 ± 1.38% in humans, compared with 1.58 ± 0.11% in vervets and 1.45 ± 0.13% in macaques (Welch's $F(2, 7.15) = 381.25$, $p < 0.001$). For all tracts bar the superior longitudinal fasciculus III, humans had significantly larger proportional volumes compared with monkey species ($p \leq 0.001$ *post hoc*; Table 5). The absolute volumes of all the above tracts were significantly different ($p < 0.001$) between species (cingulum, $F(2, 12.97) = 426.31$; uncinate, $F(2, 11.50) = 113.89$; frontal aslant tract, $F(2, 13.44) = 122.03$; superior longitudinal fasciculus branch I, $F(2, 12.80) = 110.79$; branch II, $F(2, 11.15) = 108.714$; branch III ,$F(2, 9.28) = 98.28$; inferior fronto-occipital fasciculus, $F(2, 13.39) = 369.15$; arcuate fasciculus, $F(2, 12.83) = 214.42$). The *post hoc* analysis shows that humans have significantly greater volume in all tracts than monkeys, and no significant differences between vervets and macaques (Table 5).

Finally, we evaluated *in vivo* and *ex vivo* differences in our tractography volume measurements of the above tracts in macaques (Fig. 6, Table 6). We found no significant differences in volume proportions between *in vivo* and *ex vivo* macaques for the majority of tracts, including the cingulum, where the volume fraction in *in vivo* monkeys was 3.65 ± 0.61%, uncinate fasciculus, 3.09 ± 0.83%, frontal aslant tract, 3.20 ± 0.48% and superior longitudinal fasciculus, where the volume proportion was 1.75 ± 0.74%, 1.29 ± 0.61% and 2.35 ± 0.36% for branches I, II and III. A significant difference was observed however for the inferior fronto-occipital fasciculus proportional volume, which was 5.76 ± 1.60% in the *in vivo* macaque data compared with 3.25 ± 0.94% in the *ex vivo* data (Welch's $F(1, 6.08) = 8.34$, $p = 0.027$). The absolute volumes were significantly different between *in* and *ex* vivo macaques in all tracts analyzed except the superior longitudinal fasciculus III. The arcuate fasciculus was not included in this statistical comparison as it was not possible to reconstruct this tract in the *in vivo* macaque datasets, possibly due to insufficient spatial resolution. To investigate inter-species differences within the same modality, we also compared human and macaque *in vivo* data (Fig. 7). Significant species differences were found in nearly all tracts, showing the same if not greater differences in tract volume proportions as seen in the human vs. *ex vivo*

monkey comparisons above. The absolute tract volumes were also significantly different between humans and *in vivo* monkeys. Statistical comparisons are detailed in Table 6.

Discussion

Two main findings emerged from our study. Firstly, the larger proportional volume of frontal connections in humans compared with monkeys is driven by association, commissural, projection and intra-frontal networks, suggesting greater communication within and between the frontal and other lobes. Secondly, within the association tracts, species-differences were driven by tracts important for motor planning, top-down visual and auditory processing, auditory memory and language. No significant differences were observed in tracts involved in emotional processing, such as the cingulum and uncinate fasciculus.

One novel dimension of our study was to consider the full extent of connections between the frontal and other lobes. Conventional voxel-based and tissue-sectioning techniques only measure white matter within the frontal lobes, whereas tractography analyzes networks extending throughout the brain. In our study, tractography revealed larger proportional volumes of local and extended frontal networks in humans compared with monkeys. This result is in line with voxel-based analyses in the present study and in the literature (Schoenemann et al., 2005; Smaers et al., 2011) and emphasizes the role of the frontal lobes in distributed networks (Smaers et al., 2017; Donahue et al., 2018). Evidence suggests that this result is driven by prefrontal rather than pre- and primary motor frontal connections (Smaers et al., 2017). Given the larger proportion of frontal white matter in humans than monkeys, we expected the converse to be true for some non-frontal tracts, as seen with the anterior commissure. This finding aligns with previous studies demonstrating a significantly smaller anterior commissure cross-sectional area in humans than monkeys (Foxman et al., 1986; Rilling and Insel, 1999).

In addition, we demonstrated that the greater proportional volume of human frontal connections was true of association, projection and commissural tract groups. This is consistent with previous reports suggesting that cortico-ponto-cerebellar connections (Ramnani et al., 2006; Smaers and Vanier, 2019), and the anterior corpus callosum (Catani and Thiebaut de Schotten, 2012) receive proportionally larger

contributions from prefrontal areas in humans compared with monkeys. Among the association pathways, greater frontal connectivity was documented in humans for both intra- and interlobar tracts, suggesting more crosstalk within and between frontal and non-frontal areas.

Furthermore, our analysis of individual long association tracts revealed unique features of human white matter connectivity, with the arcuate fasciculus showing the most striking species-differences. Non-human primates share a subcomponent of the arcuate fasciculus with humans, projecting to the posterior superior temporal gyrus, consistent with previous macaque axonal tracing (Petrides and Pandya, 2002; Schmahmann and Pandya, 2006) and diffusion imaging studies (Croxson et al., 2005; Rilling et al., 2008). This subcomponent is thought to be involved in acoustic spatiotemporal processing and stimulus identification (Aboitiz and García, 2009). However, in humans, the long segment of the arcuate fasciculus projects more anteriorly to the superior temporal gyrus and extends to the middle and inferior temporal gyri (Catani et al., 2005; Thiebaut de Schotten et al., 2012), which are proportionally larger in humans. The arcuate fasciculus links perisylvian regions involved with auditory memory (Rauschecker and Scott, 2009; Schulze et al., 2012), word learning (López-Barroso et al., 2013) and syntax (Wilson et al., 2011).

Another tract with significant differences between species was the inferior fronto-occipital fasciculus. While the functions of this tract remain largely unknown (Forkel et al., 2014), its greater proportional volume in humans may facilitate direct frontal access to visual inputs and top-down control of early visual processing for functions like face and object perception (Pins and ffytche, 2003; Bar et al., 2006), and reading (Shaywitz et al., 2002). It is important to note that the existence of this tract in monkeys is debated, and most visual associative areas in the human occipital lobe are located in temporal and parietal lobes of the monkey brain. Tractography (Mars et al., 2016; Feng et al., 2017) and blunt dissection studies (Decramer et al., 2018; Sarubbo et al., 2019) show connections between frontal and occipital lobes in monkeys, matching the trajectory of the inferior fronto-occipital fasciculus in humans (Curran, 1909). However, neither of these methods is able to distinguish mono- from polysynaptic pathways, leaving open the question of whether these pathways are direct connections, or composed of segments with lateral terminations in the temporal cortex. The question arises because many axonal tracing studies, able to identify monosynaptic pathways, have failed to reveal the inferior fronto-occipital fasciculus (Schmahmann

and Pandya, 2006; Petrides, 2013). Other macaque axonal tracing studies have revealed connections between frontal and occipital cortices (Barbas and Mesulam, 1981; Gerbella et al., 2010; Markov et al., 2014), however their methods are not sensitive to axonal trajectories and do not report whether these axons follow the course expected for the inferior fronto-occipital fasciculus. Further investigation is required to resolve this issue.

Differences in the superior longitudinal fasciculus were also significant. These fronto-parietal tracts are involved in motor cognition (Duffy and Burchfiel, 1971; Leiguarda and Marsden, 2000; Parlatini et al., 2017) and visuospatial attention (Corbetta et al., 2002; Picard and Strick, 2003; Buschman and Miller, 2007; Goldenberg and Spatt, 2009; Thiebaut de Schotten et al., 2011; Parlatini et al., 2017). Their damage manifests with visuospatial neglect (Beis et al., 2004; Thiebaut de Schotten et al., 2014) and impaired reaching and grasping in humans and monkeys (Leiguarda and Marsden, 2000), suggesting common functions across species. Indeed the superior longitudinal fasciculus provides parietal input to the premotor cortex (Petrides and Pandya, 1984), part of an interconnected frontal network for hand and digit movement (Dum and Strick, 2002; 2005; Howells et al., 2018), which is highly developed across primates (Hopkins and Phillips, 2017). Beyond manual dexterity, inter-species differences in this tract may be related to functions greatly developed in humans, such as tool-making (Hecht et al., 2015) and writing (Duncan, 2010; Purcell et al., 2011; Planton et al., 2013; Genovesio et al., 2014).

The lack of species differences in the uncinate fasciculus and cingulum indicates a shared anatomical substrate for these fronto-limbic tracts dedicated to aspects of memory (Gaffan and Wilson, 2008), decision making (Rushworth and Behrens, 2008) and social and emotional behavior (Rolls, 2015). Similarly, lack of differences in the frontal aslant tract, a recently described pathway between the inferior frontal gyrus and superior medial frontal cortex (Lawes et al., 2008; Catani et al., 2012b) may indicate a common substrate for vocalization or orofacial movements (Petrides et al., 2005).

To verify that interspecies differences in our results were not driven by *in – ex vivo* differences, we compared both modalities within macaques, and investigated species differences with *in vivo* data. The *in – ex vivo* comparison showed overall agreement in proportional volume, while absolute volume was greater

in vivo, possibly due to *ex vivo* tissue shrinkage or greater partial volume effects in the lower resolution *in vivo* datasets. Our comparison of *in vivo* human and macaque data showed similar interspecies differences to the main results. We therefore favored using *ex vivo* monkey datasets in our analysis over lower resolution *in vivo* data, to maximize our ability to resolve small white matter bundles in the monkey brain.

While tractography is the only method currently able to reconstruct white matter pathways *in vivo* (Dell'Acqua and Catani, 2012; Jbabdi et al., 2015), its limitations are widely acknowledged (Jones, 2010; Dell'Acqua and Catani, 2012; Dell'Acqua and Tournier, 2019). We used deterministic rather than probabilistic tractography to avoid tract length and direction biases (Jones, 2010; Liptrot et al., 2014; Donahue et al., 2016), whole brain seeding to prevent initialization point bias, and spherical deconvolution to estimate multiple fiber directions per voxel (Dell'Acqua et al., 2010; Jones, 2010; Catani et al., 2012a). To minimize false positives (Maier-Hein et al., 2016), tractography was inspected by an expert anatomist (M.C.) and streamlines with anatomically implausible trajectories manually removed.

In this paper we focused on the frontal lobe, however, other areas of association cortex play equally significant roles in human high-level functions. Temporal and parietal regions are also shown to be disproportionally larger in humans than monkeys (Van Essen and Dierker, 2007) though the prefrontal cortex appears to show the greatest difference (Smaers et al., 2017). Accordingly in our results, the frontal tracts with the greatest species-differences in volume proportion were those connecting with temporal, parietal and occipital areas. In future, the networks of other lobes should be studied more fully to understand differences between human and non-human primates (Catani et al., 2017).

In conclusion, diffusion tractography revealed greater proportional volume of frontal white matter networks in humans compared with monkeys, with significant differences for association, commissural, projection and intra-frontal networks. Striking interspecies differences were found for the arcuate, superior longitudinal and inferior fronto-occipital fasciculi. Other frontal association tracts and one non-frontal limbic tract, the anterior commissure, occupied similar or smaller volume proportions in humans compared with monkeys. While unable to make inferences about evolution directly, these results support the hypothesis of rearrangement of whole brain connectivity during human evolution. This pattern of long-

458 range frontal connectivity in humans may have resulted from reduced reliance on certain limbic functions,
459 increased feed-forward relay of sensory inputs and direct top-down modulation of early perceptual
460 processing necessary for the development of higher cognitive functions.

461 **References**

462
463 Aboitiz F, García R (2009) Merging of phonological and gestural circuits in early language evolution. Rev
464 Neurosci 20:71–84.

465 Andersson JLR, Skare S, Ashburner J (2003) How to correct susceptibility distortions in spin-echo echo-
466 planar images: application to diffusion tensor imaging. Neuroimage 20:870–888.

467 Andersson JLR, Sotiropoulos SN (2016) An integrated approach to correction for off-resonance effects and
468 subject movement in diffusion MR imaging. Neuroimage 125:1063–1078.

469 Avants BB, Tustison NJ, Song G, Cook PA, Klein A, Gee JC (2011) A reproducible evaluation of ANTs
470 similarity metric performance in brain image registration. Neuroimage 54:2033–2044.

471 Bar M, Kassam KS, Ghuman AS, Boshyan J, Schmid AM, Schmidt AM, Dale AM, Hämäläinen MS,
472 Marinkovic K, Schacter DL, Rosen BR, Halgren E (2006) Top-down facilitation of visual recognition.
473 Proc Natl Acad Sci USA 103:449–454.

474 Barbas H, Mesulam MM (1981) Organization of afferent input to subdivisions of area-8 in the Rhesus-
475 Monkey. J Comp Neurol Psychol 200:407–431.

476 Barton RA, Venditti C (2013) Human frontal lobes are not relatively large. Proc Natl Acad Sci USA
477 110:9001–9006.

478 Beis J-M et al. (2004) Right spatial neglect after left hemisphere stroke: qualitative and quantitative study.
479 Neurology 63:1600–1605.

480 Buschman TJ, Miller EK (2007) Top-down versus bottom-up control of attention in the prefrontal and
481 posterior parietal cortices. Science 315:1860–1862.

482 Catani M, Bodi I, Dell'Acqua F (2012a) Comment on "The geometric structure of the brain fiber
483 pathways". Science 337:1605.

484 Catani M, Dell'Acqua F, Vergani F, Malik F, Hodge H, Roy P, Valabregue R, Thiebaut de Schotten M
485 (2012b) Short frontal lobe connections of the human brain. Cortex 48:273–291.

486 Catani M, Howard RJ, Pajevic S, Jones DK (2002) Virtual in vivo interactive dissection of white matter
487 fasciculi in the human brain. Neuroimage 17:77–94.

488 Catani M, Jones DK, ffytche DH (2005) Perisylvian language networks of the human brain. Ann Neurol
489 57:8–16.

490 Catani M, Robertsson N, Beyh A, Huynh V, de Santiago Requejo F, Howells H, Barrett RLC, Aiello M,
491 Cavaliere C, Dyrby TB, Krug K, Ptito M, D'Arceuil H, Forkel SJ, Dell'Acqua F (2017) Short parietal
492 lobe connections of the human and monkey brain. Cortex 97:339–357.

493 Catani M, Thiebaut de Schotten M (2012) Atlas of human brain connections. Oxford: Oxford University
494 Press.

495 Cerliani L, D'Arceuil H, Thiebaut de Schotten M (2016) Connectivity-based parcellation of the macaque
496 frontal cortex, and its relation with the cytoarchitectonic distribution described in current atlases. Brain
497 Struct Funct 222:1–19.

498 Clinch JJ, Keselman HJ (1982) Parametric alternatives to the analysis of variance. J Educ Stat 7:207–214.

499 Collins DL, Zijdenbos AP, Baaré WFC, Evans AC (1999) ANIMAL+INSECT: Improved cortical structure
500 segmentation. In: Similarity-Based Pattern Recognition (Pelillo M, Hancock ER, eds), pp 210–223
501 Lecture Notes in Computer Science. Berlin, Heidelberg: Springer.

502 Corbetta M, Kincade JM, Shulman GL (2002) Neural systems for visual orienting and their relationships to
503 spatial working memory. J Cogn Neurosci 14:508–523.

504 Croxson PL, Johansen-Berg H, Behrens TEJ, Robson MD, Pinsk MA, Gross CG, Richter W, Richter MC,
505 Kastner S, Rushworth MFS (2005) Quantitative investigation of connections of the prefrontal cortex in
506 the human and macaque using probabilistic diffusion tractography. J Neurosci 25:8854–8866.

507 Curran EJ (1909) A new association fiber tract in the cerebrum with remarks on the fiber tract dissection
508 method of studying the brain. J Comp Neurol Psychol 19:645–656.

509 de Crespigny AJ, D'Arceuil HE, Maynard KI, He J, McAuliffe D, Norbash A, Sehgal PK, Hamberg L,
510 Hunter G, Budzik RF, Putman CM, Gonzalez RG (2005) Acute studies of a new primate model of
511 reversible middle cerebral artery occlusion. J Stroke Cerebrovasc Dis 14:80–87.

512 Decramer T, Swinnen S, van Loon J, Janssen P, Theys T (2018) White matter tract anatomy in the rhesus
513 monkey: a fiber dissection study. Brain Struct Funct 223:3681–3688.

514 Dell'Acqua F, Catani M (2012) Structural human brain networks: hot topics in diffusion tractography. Curr
515 Opin Neurol 25:375–383.

516 Dell'Acqua F, Lacerda L, Catani M, Simmons A (2014) Anisotropic Power Maps: A diffusion contrast to
517 reveal low anisotropy tissues from HARDI data. In, pp 29960–29967. Milan, Italy.

518 Dell'Acqua F, Scifo P, Rizzo G, Catani M, Simmons A, Scotti G, Fazio F (2010) A modified damped
519 Richardson-Lucy algorithm to reduce isotropic background effects in spherical deconvolution.
520 Neuroimage 49:1446–1458.

521 Dell'Acqua F, Simmons A, Williams SCR, Catani M (2013) Can spherical deconvolution provide more
522 information than fiber orientations? Hindrance modulated orientational anisotropy, a true-tract specific
523 index to characterize white matter diffusion. Hum Brain Mapp 34:2464–2483.

524 Dell'Acqua F, Tournier J-D (2019) Modelling white matter with spherical deconvolution: how and why?
525 NMR Biomed 32:e3945.

526 Donahue CJ, Glasser MF, Preuss TM, Rilling JK, Van Essen DC (2018) Quantitative assessment of
527 prefrontal cortex in humans relative to nonhuman primates. Proc Natl Acad Sci USA 115:E5183–
528 E5192.

529 Donahue CJ, Sotiropoulos SN, Jbabdi S, Hernandez-Fernandez M, Behrens TEJ, Dyrby TB, Coalson T,
530 Kennedy H, Knoblauch K, Van Essen DC, Glasser MF (2016) Using diffusion tractography to predict
531 cortical connection strength and distance: a quantitative comparison with tracers in the monkey. J
532 Neurosci 36:6758–6770.

533 Duffy FH, Burchfiel JL (1971) Somatosensory system: organizational hierarchy from single units in
534 monkey area 5. Science 172:273–275.

535 Dum R, Strick P (2002) Motor areas in the frontal lobe of the primate. Physiology & Behavior 77:677–682.

536 Dum RP, Strick PL (2005) Frontal lobe inputs to the digit representations of the motor areas on the lateral
537 surface of the hemisphere. J Neurosci 25:1375–1386.

538 Duncan J (2010) The multiple-demand (MD) system of the primate brain: mental programs for intelligent
539 behaviour. Trends Cogn Sci 14:172–179.

540 Dyrby TB, Baaré WFC, Alexander DC, Jelsing J, Garde E, Søgaard LV (2011) An ex vivo imaging
541 pipeline for producing high-quality and high-resolution diffusion-weighted imaging datasets. Hum
542 Brain Mapp 32:544–563.

543 Dyrby TB, Søgaard LV, Parker GJM, Alexander DC, Lind NM, Baaré WFC, Hay-Schmidt A, Eriksen N,
544 Pakkenberg B, Paulson OB, Jelsing J (2007) Validation of in vitro probabilistic tractography.
545 Neuroimage 37:1267–1277.

546 D'Arceuil HE, Westmoreland S, de Crespigny AJ (2007) An approach to high resolution diffusion tensor
547 imaging in fixed primate brain. Neuroimage 35:553–565.

548 Feng L, Jeon T, Yu Q, Ouyang M, Peng Q, Mishra V, Pletikos M, Sestan N, Miller MI, Mori S, Hsiao S,
549 Liu S, Huang H (2017) Population-averaged macaque brain atlas with high-resolution ex vivo DTI
550 integrated into in vivo space. Brain Struct Funct 222:4131–4147.

551 Fonov V, Evans AC, Botteron K, Almli CR, McKinstry RC, Collins DL (2011) Unbiased average age-
552 appropriate atlases for pediatric studies. Neuroimage 54:313–327.

553 Fonov VS, Evans AC, McKinstry RC, Almli CR, Collins DL (2009) Unbiased nonlinear average age-
554 appropriate brain templates from birth to adulthood. Neuroimage 47:S102.

555 Forkel SJ, Thiebaut de Schotten M, Kawadler JM, Dell'Acqua F, Danek A, Catani M (2014) The anatomy
556 of fronto-occipital connections from early blunt dissections to contemporary tractography. Cortex
557 56:73–84.

558 Foxman BT, Oppenheim J, Petito CK, Gazzaniga MS (1986) Proportional anterior commissure area in
559 humans and monkeys. Neurology 36:1513–1517.

560 Fuster JM (1988) Prefrontal cortex. In: Comparative neuroscience and neurobiology (Irwin LN, ed), pp
561 107–109. Boston, MA,: Birkhäuser.

562 Gabi M, Neves K, Masseron C, Ribeiro PFM, Ventura-Antunes L, Torres L, Mota B, Kaas JH, Herculano-
563 Houzel S (2016) No relative expansion of the number of prefrontal neurons in primate and human
564 evolution. Proc Natl Acad Sci USA 113:9617–9622.

565 Gaffan D, Wilson C (2008) Medial temporal and prefrontal function: recent behavioural disconnection
566 studies in the macaque monkey. Cortex 44:928–935.

567 Games PA, Howell JF (1976) Pairwise multiple comparison procedures with unequal n's and/or variances:
568 a Monte Carlo study. J Educ Stat 1:113–125.

569 Genovesio A, Wise SP, Passingham RE (2014) Prefrontal–parietal function: from foraging to foresight.
570 Trends Cogn Sci 18:72–81.

571 Gerbella M, Belmalih A, Borra E, Rozzi S, Luppino G (2010) Cortical connections of the macaque caudal
572 ventrolateral prefrontal areas 45A and 45B. Cereb Cortex 20:141–168.

573 Goldenberg G, Spatt J (2009) The neural basis of tool use. Brain 132:1645–1655.

574 Hecht EE, Gutman DA, Bradley BA, Preuss TM, Stout D (2015) Virtual dissection and comparative
575 connectivity of the superior longitudinal fasciculus in chimpanzees and humans. Neuroimage
576 108:124–137.

577 Hopkins WD, Phillips KA (2017) Noninvasive imaging technologies in primates. In: Lateralized brain
578 functions (Rogers L, Vallortigara G, eds), pp 441–470 Neuromethods. New York, NY: Humana Press.

579 Howells H, Thiebaut de Schotten M, Dell'Acqua F, Beyh A, Zappalà G, Leslie A, Simmons A, Murphy
580 DGM, Catani M (2018) Frontoparietal tracts linked to lateralized hand preference and manual
581 specialization. Cereb Cortex 28:2482–2494.

582 Jbabdi S, Lehman JF, Haber SN, Behrens TEJ (2013) Human and monkey ventral prefrontal fibers use the
583 same organizational principles to reach their targets: tracing versus tractography. J Neurosci 33:3190–
584 3201.

585 Jbabdi S, Sotiropoulos SN, Haber SN, Van Essen DC, Behrens TEJ (2015) Measuring macroscopic brain
586 connections in vivo. Nat Neurosci 18:1546–1555.

587 Jones DK (2010) Challenges and limitations of quantifying brain connectivity in vivo with diffusion MRI.
588 Imaging Med 2:341-355.

589 Large I, Bridge H, Ahmed B, Clare S, Kolasinski J, Lam WW, Miller KL, Dyrby TB, Parker AJ, Smith
590 JET, Daubney G, Sallet J, Bell AH, Krug K (2016) Individual differences in the alignment of
591 structural and functional markers of the V5/MT complex in primates. Cereb Cortex 26:3928–3944.

592 Lawes INC, Barrick TR, Murugam V, Spierings N, Evans DR, Song M, Clark CA (2008) Atlas-based
593 segmentation of white matter tracts of the human brain using diffusion tensor tractography and
594 comparison with classical dissection. Neuroimage 39:62–79.

595 Leiguarda RC, Marsden CD (2000) Limb apraxias: higher-order disorders of sensorimotor integration.
596 Brain 123:860–879.

597 Liptrot MG, Sidaros K, Dyrby TB (2014) Addressing the path-length-dependency confound in white matter
598 tract segmentation. PLoS ONE 9: e96247.

599 López-Barroso D, Catani M, Ripollés P, Dell'Acqua F, Rodriguez-Fornells A, de Diego-Balaguer R (2013)
600 Word learning is mediated by the left arcuate fasciculus. Proc Natl Acad Sci USA 110:13168–13173.

601 Maier-Hein KH, et al (2017) The challenge of mapping the human connectome based on diffusion
602 tractography. Nature Communications 8:1349.

603 Markov NT, Ercsey-Ravasz MM, Ribeiro Gomes AR, Lamy C, Magrou L, Vezoli J, Misery P, Falchier
604 A, Quilodran R, Gariel MA, Sallet J, Gamanut R, Huissoud C, Clavagnier S, Giroud P, Sappey-
605 Marinier D, Barone P, Dehay C, Toroczkai Z, Knoblauch K, Van Essen DC, Kennedy H (2014) A
606 weighted and directed interareal connectivity matrix for macaque cerebral cortex. Cereb Cortex
607 24:17–36.

608 Mars RB, Foxley S, Verhagen L, Jbabdi S, Sallet J, Noonan MP, Neubert F-X, Andersson JLR, Croxson
609 PL, Dunbar RIM, Khrapitchev AA, Sibson NR, Miller KL, Rushworth MFS (2016) The extreme
610 capsule fiber complex in humans and macaque monkeys: a comparative diffusion MRI tractography

611 study. Brain Struct Funct 221:4059–4071.

612 Mars RB, Jbabdi S, Sallet J, O'Reilly JX, Croxson PL, Olivier E, Noonan MP, Bergmann C, Mitchell AS,
613 Baxter MG, Behrens TEJ, Johansen-Berg H, Tomassini V, Miller KL, Rushworth MFS (2011)
614 Diffusion-weighted imaging tractography-based parcellation of the human parietal cortex and
615 comparison with human and macaque resting-state functional connectivity. J Neurosci 31:4087–4100.

616 Parlatini V, Radua J, Dell'Acqua F, Leslie A, Simmons A, Murphy DGM, Catani M, Thiebaut de Schotten
617 M (2017) Functional segregation and integration within fronto-parietal networks. Neuroimage
618 146:367–375.

619 Passingham RE, Wise SP (2012) The Neurobiology of the prefrontal cortex. Oxford: Oxford University
620 Press.

621 Petrides M (2013) Neuroanatomy of language regions of the human brain. San Diego: Academic Press.

622 Petrides M, Cadoret G, Mackey S (2005) Orofacial somatomotor responses in the macaque monkey
623 homologue of Broca's area. Nature 435:1235–1238.

624 Petrides M, Pandya DN (1984) Projections to the frontal cortex from the posterior parietal region in the
625 rhesus monkey. J Comp Neurol Psychol 228:105–116.

626 Petrides M, Pandya DN (2002) Comparative cytoarchitectonic analysis of the human and the macaque
627 ventrolateral prefrontal cortex and corticocortical connection patterns in the monkey. Eur J Neurosci
628 16:291–310.

629 Picard N, Strick PL (2003) Activation of the supplementary motor area (SMA) during performance of
630 visually guided movements. Cereb Cortex 13:977–986.

631 Pins D, ffytche DH (2003) The neural correlates of conscious vision. Cereb Cortex 13:461–474.

632 Planton S, Jucla M, Roux F-E, Démonet J-F (2013) The “handwriting brain”: a meta-analysis of
633 neuroimaging studies of motor versus orthographic processes. Cortex 49:2772–2787.

634 Purcell JJ, Turkeltaub PE, Eden GF, Rapp B (2011) Examining the central and peripheral processes of
635 written word production through meta-analysis. Front Psychol 2:239.

636 Ramnani N, Behrens TEJ, Johansen-Berg H, Richter MC, Pinsk MA, Andersson JLR, Rudebeck P,
637 Ciccarelli O, Richter W, Thompson AJ, Gross CG, Robson MD, Kastner S, Matthews PM (2006) The
638 evolution of prefrontal inputs to the cortico-pontine system: diffusion imaging evidence from Macaque
639 monkeys and humans. Cereb Cortex 16:811–818.

640 Rauschecker JP, Scott SK (2009) Maps and streams in the auditory cortex: nonhuman primates illuminate
641 human speech processing. Nat Neurosci 12:718–724.

642 Rilling JK, Glasser MF, Preuss TM, Ma X, Zhao T, Hu X, Behrens TEJ (2008) The evolution of the arcuate
643 fasciculus revealed with comparative DTI. Nat Neurosci 11:426–428.

644 Rilling JK, Insel TR (1999) Differential expansion of neural projection systems in primate brain evolution.
645 Neuroreport 10:1453–1459.

646 Rohlfing T, Kroenke CD, Sullivan EV, Dubach MF, Bowden DM, Grant KA, Pfefferbaum A (2012) The
647 INIA19 template and NeuroMaps atlas for primate brain image parcellation and spatial normalization.
648 Front Neuroinform 6:27.

649 Rolls ET (2015) Limbic systems for emotion and for memory, but no single limbic system. Cortex 62:119–
650 157.

651 Rushworth MFS, Behrens TEJ (2008) Choice, uncertainty and value in prefrontal and cingulate cortex. Nat
652 Neurosci 11:389–397.

653 Sarubbo S, Petit L, De Benedictis A, Chioffi F, Ptito M, Dyrby TB (2019) Uncovering the inferior fronto-
654 occipital fascicle and its topological organization in non-human primates: the missing connection for
655 language evolution. Brain Struct Funct 9:381–15.

656 Schmahmann JD, Pandya DN (2006) Fiber pathways of the brain. New York: Oxford University Press.

657 Schoenemann PT, Sheehan MJ, Glotzer LD (2005) Prefrontal white matter volume is disproportionately
658 larger in humans than in other primates. Nat Neurosci 8:242–252.

659 Schulze K, Vargha-Khadem F, Mishkin M (2012) Test of a motor theory of long-term auditory memory.
660 Proc Natl Acad Sci USA 109:7121–7125.

661 Semendeferi K, Lu A, Schenker NM, Damásio H (2002) Humans and great apes share a large frontal
662 cortex. Nat Neurosci 5:272–276.

663 Shaywitz BA, Shaywitz SE, Pugh KR, Mencl WE, Fulbright RK, Skudlarski P, Constable RT, Marchione
664 KE, Fletcher JM, Lyon GR, Gore JC (2002) Disruption of posterior brain systems for reading in
665 children with developmental dyslexia. Biol Psychiatry 52:101–110.

666 Sherwood CC, Smaers JB (2013) What's the fuss over human frontal lobe evolution? Trends Cogn Sci
667 17:432–433.

668 Smaers JB, Gómez-Robles A, Parks AN, Sherwood CC (2017) Exceptional evolutionary expansion of
669 prefrontal cortex in great apes and humans. Curr Biol 27:714–720.

670 Smaers JB, Schleicher A, Zilles K, Vinicius L (2010) Frontal white matter volume is associated with brain
671 enlargement and higher structural connectivity in anthropoid primates. PLoS ONE 5:e9123.

672 Smaers JB, Steele J, Case CR, Cowper A, Amunts K, Zilles K (2011) Primate prefrontal cortex evolution:
673 human brains are the extreme of a lateralized ape trend. Brain Behav Evol 77:67–78.

674 Smaers JB, Vanier DR (2019) Brain size expansion in primates and humans is explained by a selective
675 modular expansion of the cortico-cerebellar system. Cortex 118:292–305.

676 Thiebaut de Schotten M, Dell'Acqua F, Forkel SJ, Simmons A, Vergani F, Murphy DGM, Catani M (2011)
677 A lateralized brain network for visuospatial attention. Nat Neurosci 14:1245–1246.

678 Thiebaut de Schotten M, Dell'Acqua F, Valabregue R, Catani M (2012) Monkey to human comparative
679 anatomy of the frontal lobe association tracts. Cortex 48:82–96.

680 Thiebaut de Schotten M, Tomaiuolo F, Aiello M, Merola S, Silvetti M, Lecce F, Bartolomeo P, Doricchi F
681 (2014) Damage to white matter pathways in subacute and chronic spatial neglect: a group study and 2
682 single-case studies with complete virtual in vivo tractography dissection. Cereb Cortex 24:691–706.

683 Van Essen DC, Dierker DL (2007) Surface-based and probabilistic atlases of primate cerebral cortex.
684 Neuron 56:209–225.

685 Welch BL (1951) On the comparison of several mean values: an alternative approach. Biometrika 38:330–
686 336.

687 Wilson SW, Galantucci S, Tartaglia MC, Rising K, Patterson DK, Henry ML, Ogar JM, DeLeon J, Miller
688 BL, Gorno-Tempini ML (2011) Syntactic processing depends on dorsal language tracts. Neuron
689 72:397–403.

690 Zhang K, Sejnowski TJ (2000) A universal scaling law between gray matter and white matter of cerebral
691 cortex. Proc Natl Acad Sci USA 97:5621–5626.

692

693 **Figure Legends**

694 **Figure 1. Pipeline for dissection of the association, commissural, projection and intra-frontal**
695 **tracts, illustrated in a single macaque brain.** A) An inclusion region of the whole left or right hemisphere
696 was used to extract all hemispheric connections. Exclusion regions (not pictured) were used to remove
697 artefactual streamlines coursing through the contralateral internal, external and extreme capsules. B) From
698 the set of streamlines in each hemisphere defined in A), an inclusion region of the frontal lobe was used to
699 select only streamlines passing through the frontal lobe, including those extending between frontal and non-
700 frontal regions. These frontal lobe connections were then further separated into the following groups: C)
701 association fibers, using an inclusion region of the frontal lobe (1) and exclusion regions in the midsagittal
702 section (2) and the subcortical nuclei (3); D) commissural fibers, using the two frontal lobes (1, 2) as
703 inclusion regions; E) projection fibers, using one inclusion region of the frontal lobe (1) and one in the
704 brainstem and thalamus (2); and F) intra-frontal association fibers. Intra-frontal fibers were defined with the
705 condition that both ends of the streamline must be within the frontal lobe region of interest. The same
706 approach was used in all species.

707 **Figure 2. Regions of interest used to dissect individual tracts in the human (left) and monkey**
708 **(right) brain.** For each example, 3D reconstructions and 2D sections are shown. In addition to the regions
709 depicted here, exclusion regions were used in the midsagittal plane, brainstem, subcortical nuclei and
710 internal capsule to exclude commissural and projection tracts, and remove individual spurious streamlines.
711 A) Uncinate fasciculus (lateral view): inclusion regions of interest are placed in the anterior temporal lobe
712 (pink) and external/extreme capsules (orange). B) Cingulum (medial view): a single inclusion region (pink)
713 on multiple coronal slices along the cingulate gyrus is used, to ensure that the superior projections of the
714 dorsal cingulum are included. C) Frontal aslant tract (anterior view): an inclusion region (light blue) is
715 placed in the white matter medial to the inferior frontal gyrus in the sagittal plane. In humans, a second
716 inclusion region (yellow) is placed in the white matter inferior to the superior frontal gyrus in the axial
717 plane, while in monkeys an atlas-defined region of the superior frontal gyrus is used as the second inclusion
718 region, to include all streamlines projecting to the medial frontal regions. Exclusion regions were then
719 placed in the frontal pole. D) Superior longitudinal fasciculus (SLF) (lateral view): one inclusion region

(yellow) is placed in the parietal lobe in line with the superior aspect of the central sulcus, and one inclusion region is used for each of the three branches, SLF I (light blue), II, (dark blue) and III (purple) all in a coronal plane passing through the precentral gyrus. Exclusion regions are used in the temporal and occipital lobe in both humans and monkeys. E) Inferior fronto-occipital fasciculus (lateral view): one inclusion region is used in the external/extreme capsules (pink) and one in the anterior border of the occipital lobe (yellow), both in the coronal plane. F) Arcuate fasciculus, long segment: in the human, one inclusion region (orange) is placed in the coronal plane just anterior to the central sulcus and one inclusion region in the axial plane inferior to the temporo-parietal junction (blue). In the monkey, to be as inclusive as possible, atlas-defined regions of the frontal lobe (pink mask) and superior temporal gyrus (yellow mask) were also used as inclusion regions of interest. In addition to the inclusion regions pictured here, exclusion regions were placed in the external/extreme capsules and the white matter of the superior temporal gyrus to remove the middle longitudinal fasciculus, and in the white matter medial to the supra-marginal gyrus to remove SLF fibers. G) Anterior commissure: two inclusion regions were used to capture the compact bundle of the anterior commissure as it crosses the midline. Each region has two slices in the sagittal plane on either side of the midline, one more medial (green), one placed more laterally (yellow). Exclusion regions were used to remove spurious streamlines forming part of the fornix, anterior thalamic projections, and other projections from the brain stem.

Figure 3. MRI methods for comparing cortical and white matter volumes across species. Images show the rescaled anatomy of representative cases and graphs display proportional and absolute volumes with mean values and data points for individual brains (H, humans n = 20; V, vervets n = 4; M, macaques n = 5). A) Voxel-based measures of frontal cortex volume. B) Voxel-based measures of frontal white matter volume. C) Tractography-based measures of frontal tracts volume. D) Tractography-based measures of anterior commissure (AC) volume. *$p < 0.05$; **$p < 0.01$; ***$p < 0.001$ when comparing humans to either vervets or macaques. For full statistical results see Results and Table 3.

Figure 4. The main tract groups compared between humans, vervets and macaques. Images show tractography reconstructions of A) the frontal association (green), B) commissural (red), C) projection (blue), and D) intralobar frontal (orange) networks in single representative brains. Graphs show

both proportional and absolute volume of each tract group, where data points represent individual brains (H, humans n = 20; V, vervets n = 4; M, macaques n =5) and species mean values are indicated by horizontal lines. *p < 0.05; **p < 0.01; ***p < 0.001 when comparing humans to either vervets or macaques. For full statistical results see Results and Table 4.

Figure 5. Comparison of the major frontal association tracts between humans, vervets and macaques. Images show tractography reconstructions from individual brains and graphs show proportional and absolute tract volume measures. Data points represent individual brains (H, humans n = 20; V, vervets n = 4; M, macaques n =5). Species means are indicated by horizontal lines. The tracts shown are: A) cingulum (burgundy color) and uncinate fasciculus (UF, dark green), which represent the major fronto-limbic association tracts; B) frontal aslant tract (FAT, pink); C) fronto-parietal connections of the superior longitudinal fasciculus (SLF I, light blue; SLF II, dark blue; SLF III, purple); D) inferior fronto-occipital fasciculus (IFOF, yellow); E) arcuate fasciculus, long segment (AF, light green). *p < 0.05; **p < 0.01; ***p < 0.001 when comparing humans to either vervets or macaques. For full statistical results see Results and Table 5.

Figure 6. Comparison of *ex vivo* and *in vivo* macaque tractography data in the macaque. Images show tractography reconstructions of A) the cingulum (burgundy) and uncinate fasciculus (UF, dark green), B) frontal aslant tract (FAT, pink), C) superior longitudinal fasciculus (SLF I, light blue; SLF II, dark blue; SLF III, purple), D) inferior fronto-occipital fasciculus (IFOF, yellow) and E) arcuate fasciculus, long segment (AF, light green). Graphs show both proportional and absolute tract volumes for individual brains species mean values. There were no significant differences in proportional tract volume between groups, except for the inferior fronto-occipital fasciculus (Welch's $F(1, 6.08) = 8.34$, *p = 0.027). The AF could not be reconstructed in the *in vivo* datasets. For full statistical results see Table 6.

Figure 7. Comparison of human and macaque *in vivo* tractography data. Images show tractography reconstructions of A) the cingulum (burgundy) and uncinate fasciculus (UF, dark green), B) frontal aslant tract (FAT, pink), C) superior longitudinal fasciculus (SLF I, light blue; SLF II, dark blue; SLF III, purple), D) inferior fronto-occipital fasciculus (IFOF, yellow) and E) arcuate fasciculus, long segment (AF, light green). Graphs show proportional and absolute tract volumes for individual brains measured from the *in vivo* dataset for both humans and monkeys. *$p < 0.05$; **$p < 0.01$; ***$p < 0.001$ when comparing humans to either vervets or macaques. Statistics were not carried out for the AF, as it was not possible to reconstruct this tract in the macaque *in vivo* datasets. For full statistical results see Table 7.

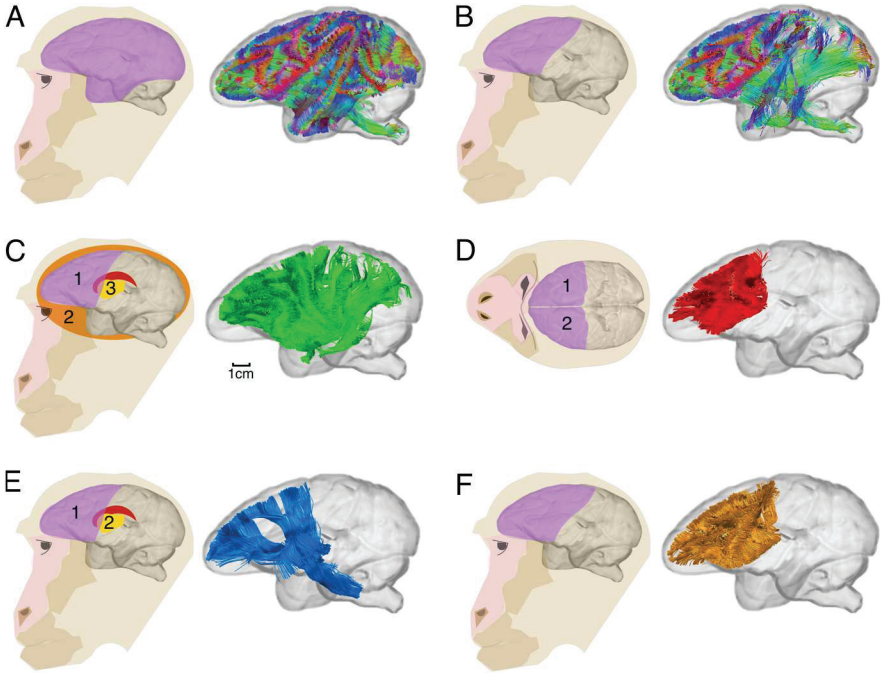

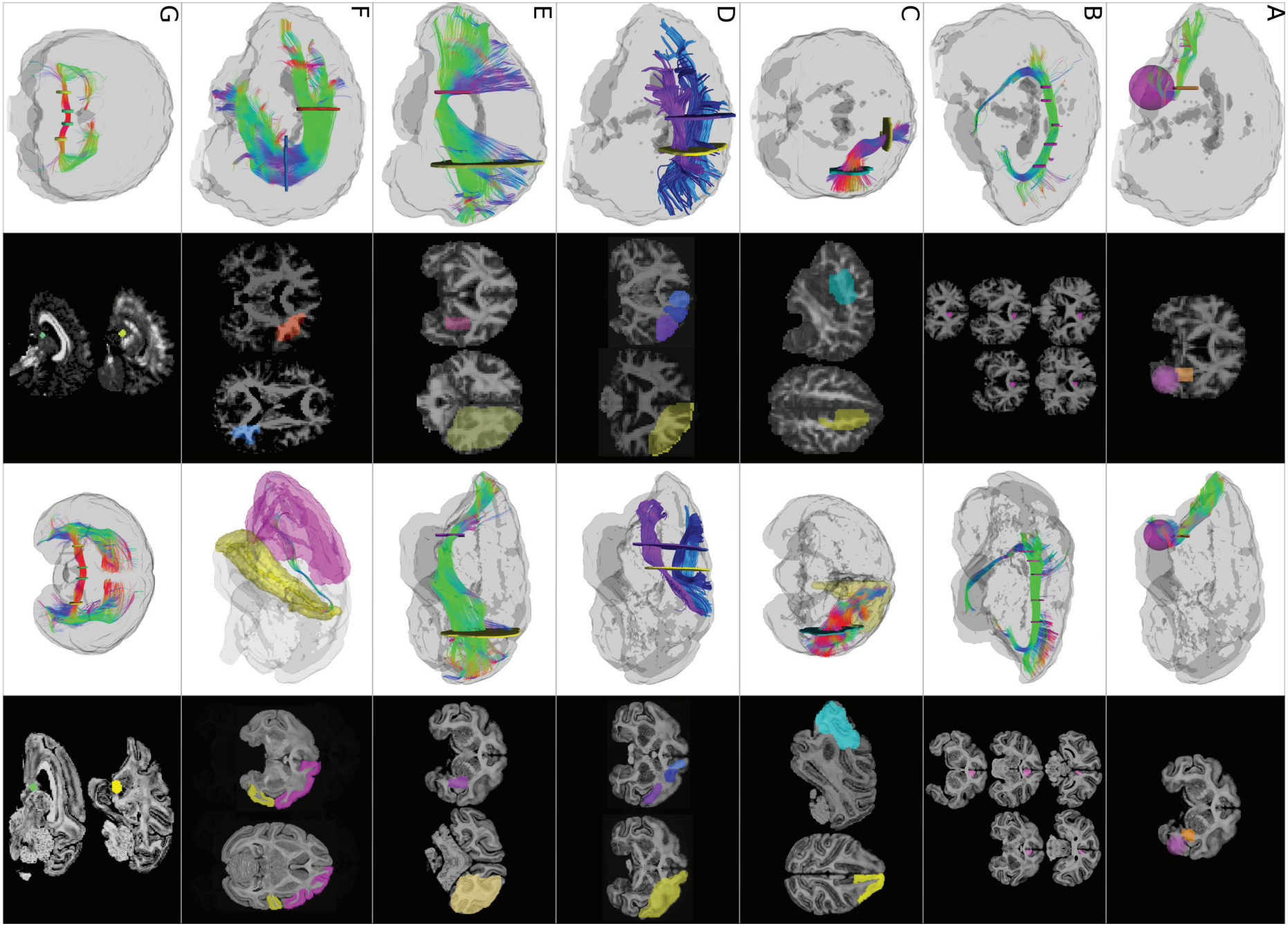

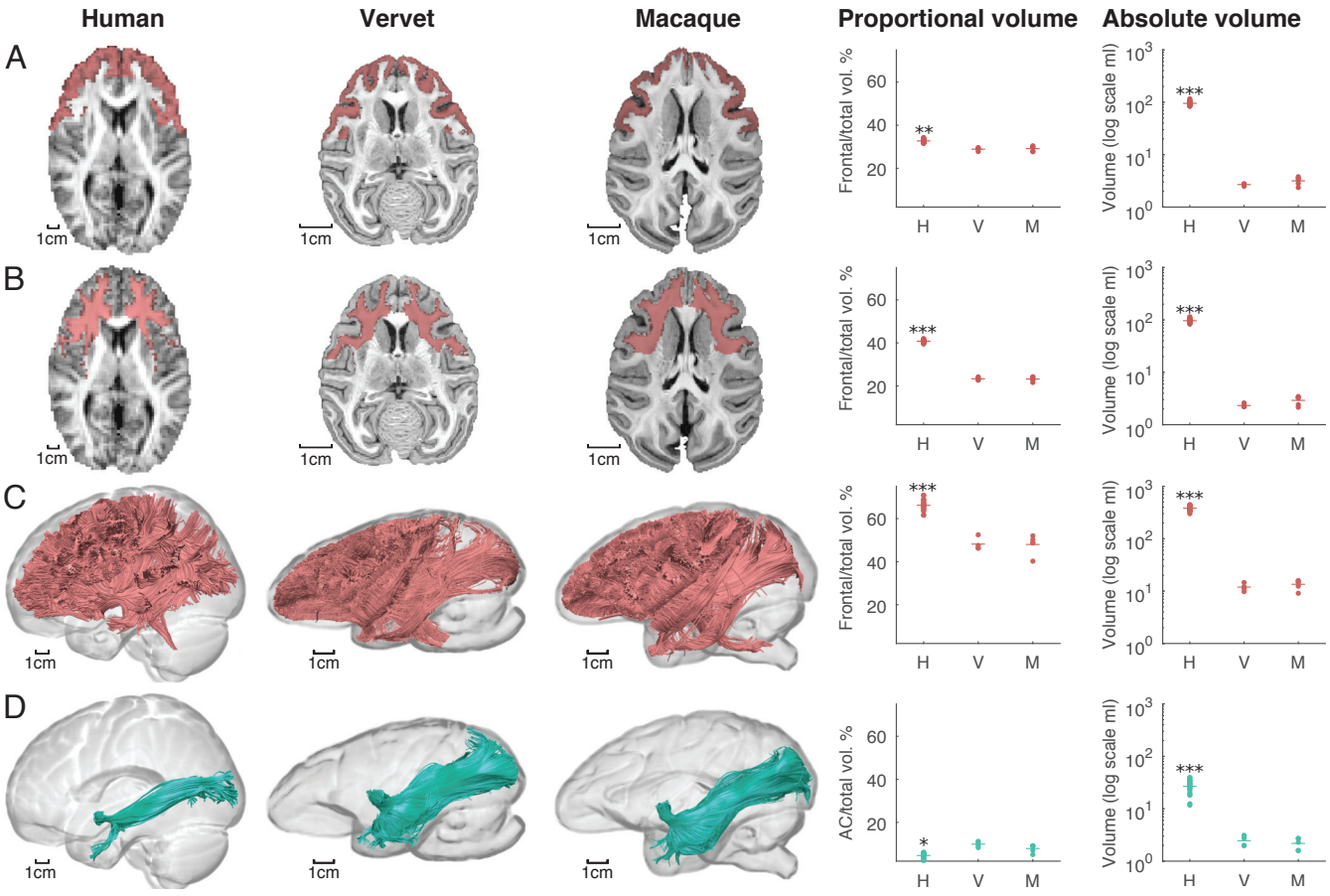

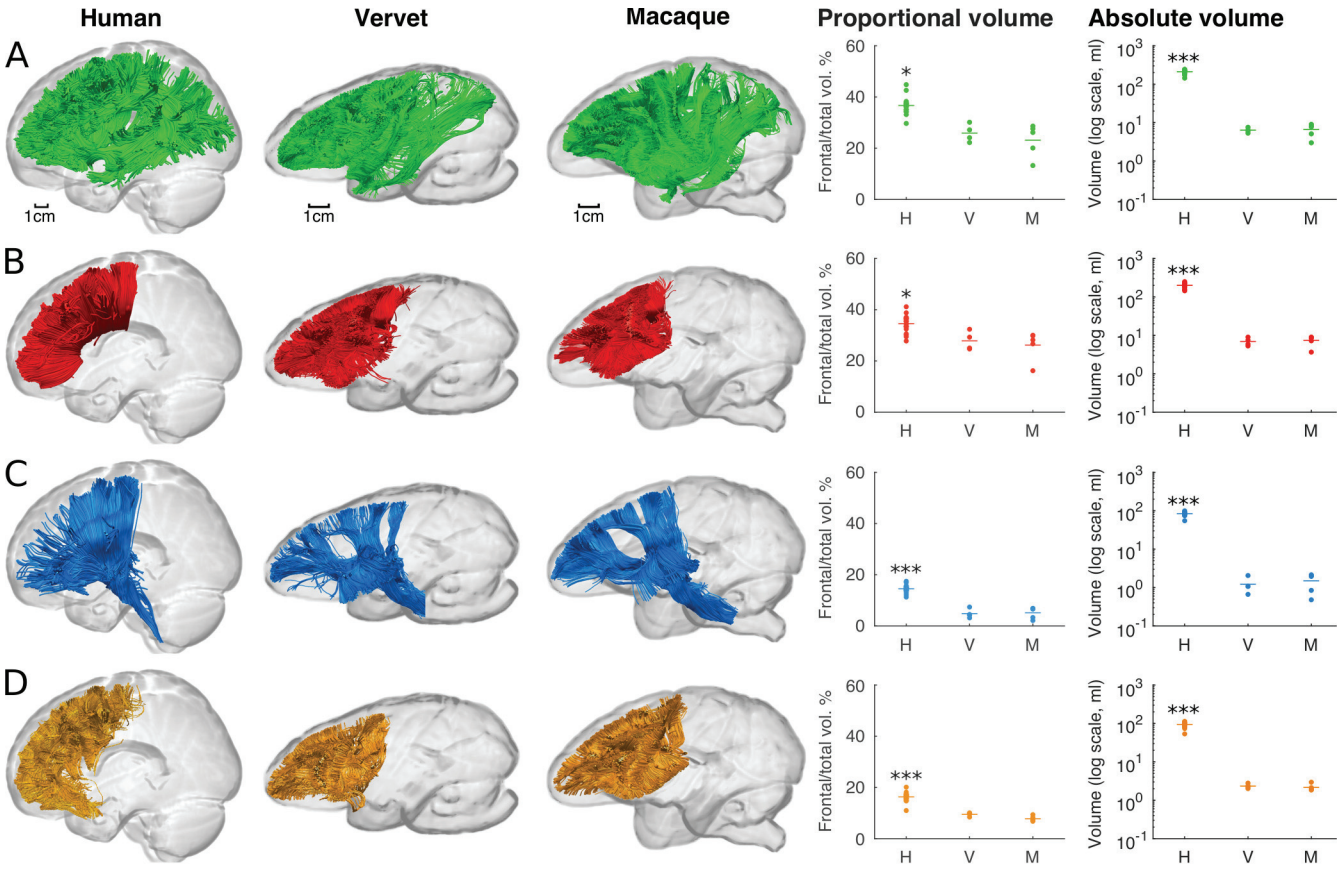

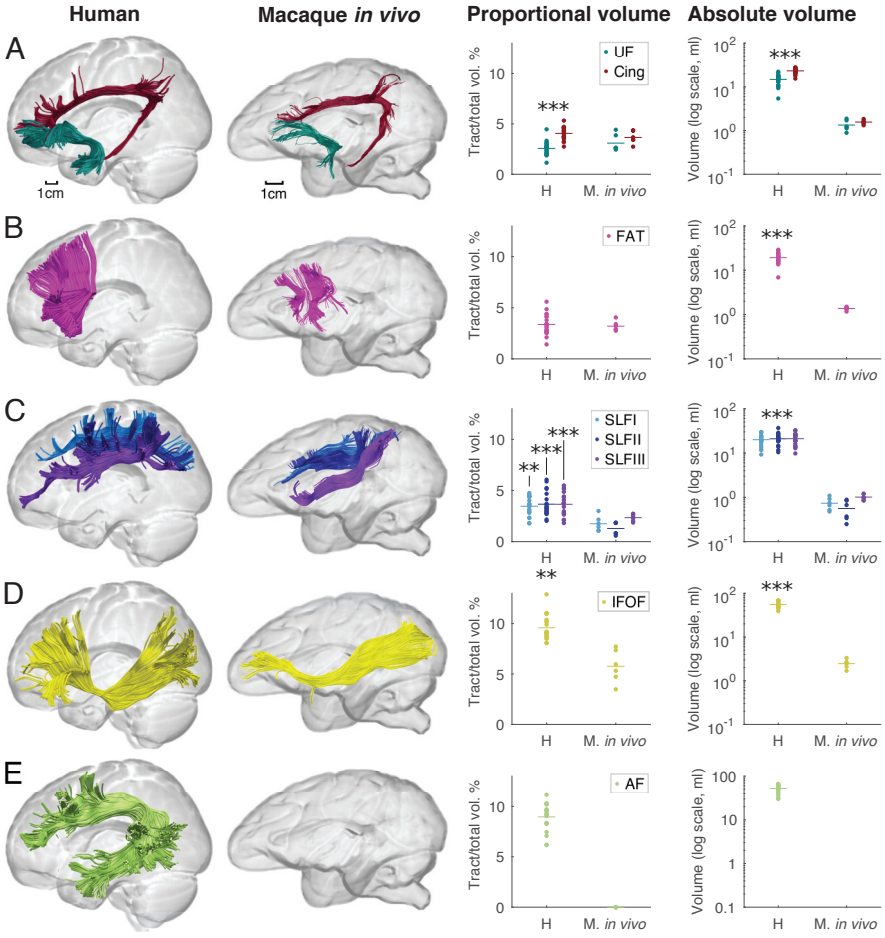

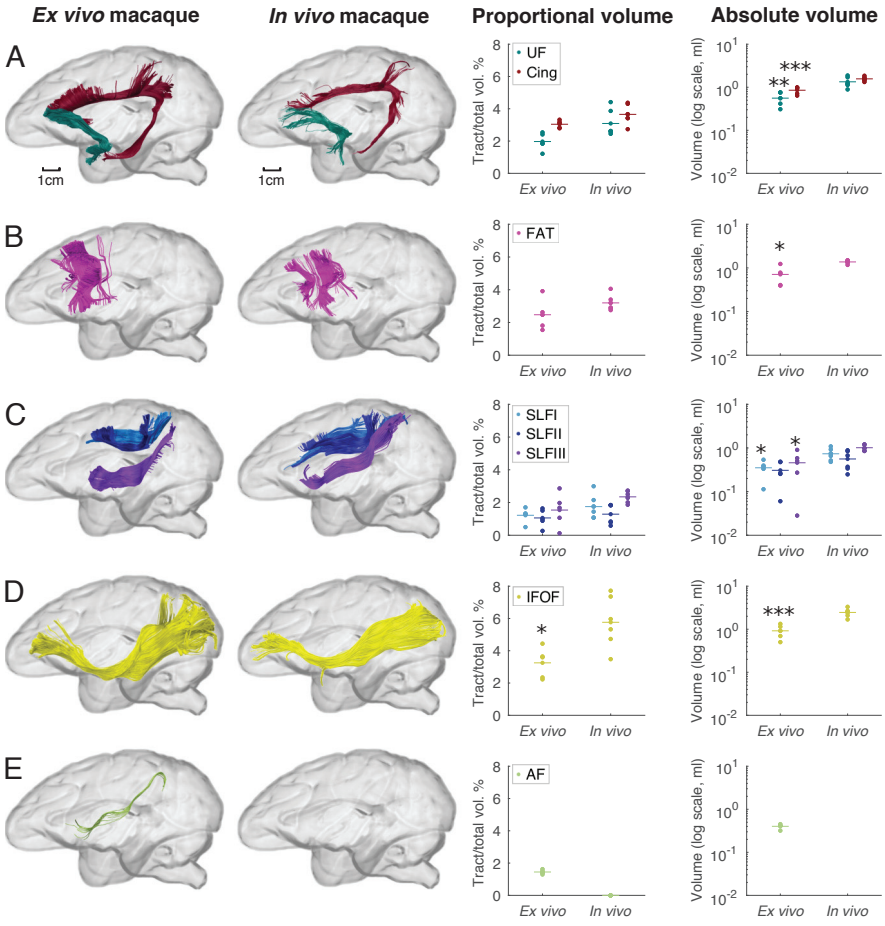

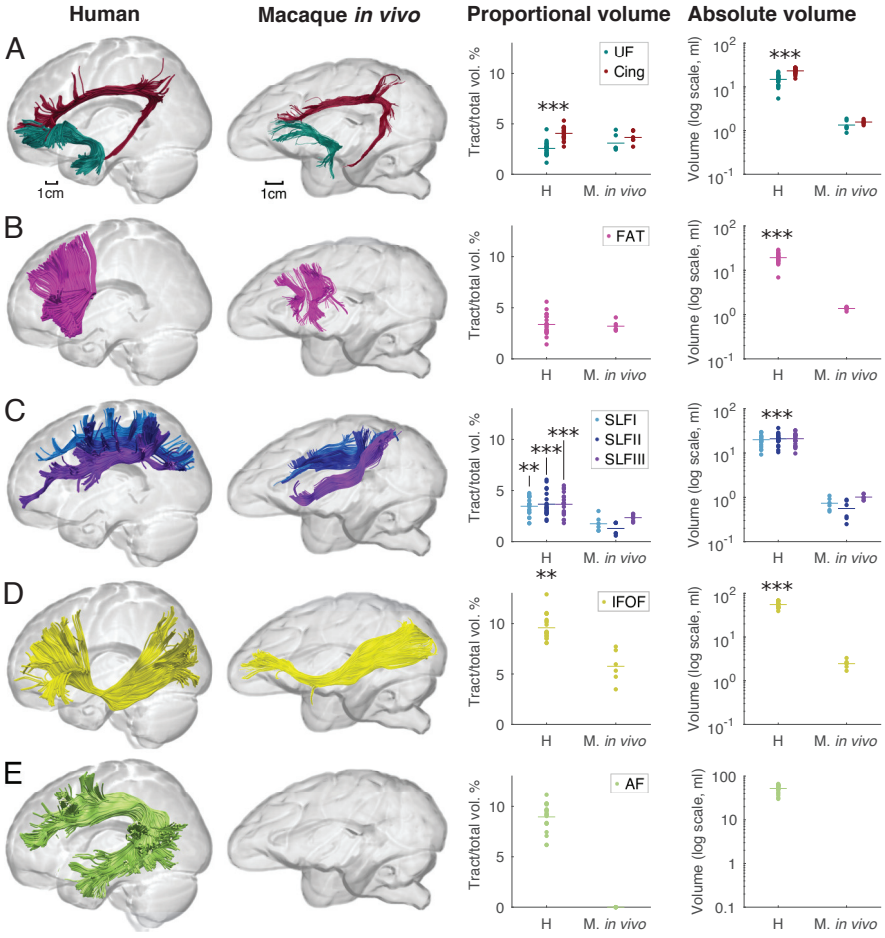

Table 1. Diffusion MRI acquisition parameters

Group	Resolution (mm^3)	b-value (s/mm^2)	b0 volumes	DWI volumes
Human	2.40 × 2.40 × 2.40	3000	7	60
Vervet 1	0.50 × 0.50 × 0.50	7660	18	256
Vervets 2-4	0.50 × 0.50 × 0.50	3151	16	87
RM	0.50 × 0.50 × 0.50	4310	3	61
CM	0.43 × 0.43 × 0.43	8000	12	119
RM *in vivo*	1.00 × 1.00 × 1.00	1500	10	80

RM: Rhesus macaque, CM: cynamologus macaque. Unless indicated, the monkey datasets were acquired *ex vivo*.

Table 2. Spherical deconvolution and tractography parameters

Group	α	No. iterations	Angle (°)	Absolute	Relative (%)	Length (mm)
Human	0.25	1000	30	0.40	4	20 – 400
Vervet 1	0.50	1000	45	0.20	5	10 – 400
Vervets 2-4	0.10	2000	45	0.20	5	10 – 400
RM	0.10	3000	45	0.20	5	10 – 400
CM 2104	0.15	2000	35	0.15	5	10 – 400
CM 2203*	0.38	2000	40	0.18	5	10 – 400
RM *in vivo*	1.00	1500	35	0.15	5	10 – 400

RM: Rhesus macaque, CM: cynamologus macaque. Unless indicated, the monkey datasets were acquired *ex vivo*. The above parameters are explained fully in Dell'Acqua et al. (2013); α, shape factor of the fiber response function; No. iterations of the spherical deconvolution algorithm; Angle, maximum angle threshold between adjacent voxels; Absolute threshold, a tractography stopping threshold based on the hindrance modulated orientational anisotropy index; Relative threshold: a stopping threshold for tractography, set to a percentage of the maximum lobe amplitude of the fiber orientation distribution function; length threshold for streamlines. * Different parameters are used to account for differences in signal to noise, which may result from varying *ex vivo* tissue quality.

Table 3. Proportional and absolute frontal volume measurements between species

Volume measures	Human (mean ± st. dev.)	Vervet	Macaque	*Post hoc* comparisons (P values)		
				Human vs vervet	Human vs macaque	Vervet vs macaque
Frontal Cortex (voxel-based)						
Proportion (%)	32.69 ± 0.79	28.89 ± 0.79	29.12 ± 1.22	0.002	0.004	0.938
Absolute (ml)	95.27 ± 8.45	2.68 ± 0.13	3.16 ± 0.57	< 0.001	< 0.001	0.271
Frontal white matter (voxel-based)						
Proportion	40.80 ± 0.62	23.33 ± 0.72	23.19 ± 1.04	< 0.001	< 0.001	0.974
Absolute	96.69 ± 7.93	2.33 ± 0.19	2.92 ± 0.59	< 0.001	< 0.001	0.182
Frontal tracts (tractography)						
Proportion	66.18 ± 2.56	48.16 ± 2.94	47.98 ± 4.54	0.001	0.001	0.997
Absolute	382.60 ± 45.30	11.91 ± 2.04	13.48 ± 2.80	< 0.001	< 0.001	0.618
Anterior commissure (tractography)						
Proportion	4.59 ± 1.15	9.90 ± 1.30	7.86 ± 1.80	0.004	0.028	0.091
Absolute	26.73 ± 7.91	2.46 ± 0.56	2.18 ± 0.56	< 0.001	< 0.001	0.754

Frontal and non-frontal (anterior commissure) volume measures in humans (n = 20), veverts (n = 4) and macaques (n = 5). Descriptive statistics and Games-Howell *post hoc* comparisons between species are given for proportional (normalized by total volume for each measure) and absolute volumes. See Results for Welch's ANOVA statistics.

Table 4. Proportional and absolute frontal tract group volume measurements between species

Tract group	Human	Vervet	Macaque	*Post hoc* comparisons (P values)		
	(mean ± st. dev.)			Human vs vervet	Human vs macaque	Vervet vs macaque
Association						
Proportion (%)	36.69 ± 3.13	25.92 ± 3.48	23.15 ± 6.46	0.010	0.018	0.706
Absolute (ml)	211.92 ± 27.19	6.36 ± 0.92	6.64 ± 2.52	< 0.001	< 0.001	0.972
Commissural						
Proportion	34.58 ± 3.30	27.85 ± 3.67	26.19 ± 5.76	0.002	0.014	0.989
Absolute	200.42 ± 32.31	6.93 ± 1.67	7.42 ± 2.22	< 0.001	< 0.001	0.924
Projection						
Proportion	14.52 ± 1.44	4.80 ± 1.82	5.14 ± 2.25	0.001	0.001	0.937
Absolute	83.60 ± 9.78	1.22 ± 0.59	1.50 ± 0.78	< 0.001	< 0.001	0.818
Intra-frontal						
Proportion	16.33 ± 1.77	9.50 ± 0.73	7.79 ± 1.04	< 0.001	< 0.001	0.055
Absolute	94.53 ± 14.68	2.34 ± 0.34	2.17 ±0.45	< 0.001	< 0.001	0.806

Association, commissural, projection and intra-frontal tract group volumes in humans (n = 20), veverts (n = 4) and macaques (n = 5). Descriptive statistics and Games-Howell *post hoc* comparisons between species are given for proportional (normalized by total volume for each measure) and absolute volumes. See Results for Welch's ANOVA statistics.

Table 5. Proportional and absolute volume measurements of frontal association tracts between species

Tract	Human (mean ± st. dev.)	Vervet	Macaque	*Post hoc* comparisons (P values)		
				Human vs vervet	Human vs macaque	Vervet vs macaque
Cingulum						
Proportion (%)	4.06 ± 0.62	3.21 ± 0.29	3.04 ± 0.23	-	-	-
Absolute (ml)	23.28 ± 3.35	0.79 ± 0.10	0.85 ± 0.16	< 0.001	< 0.001	0.760
UF						
Proportion	2.56 ± 0.69	2.38 ± 0.39	1.97 ± 0.53	-	-	-
Absolute	14.86 ± 4.11	0.58 ± 0.08	0.56 ± 0.20	< 0.001	< 0.001	0.971
FAT						
Proportion	3.37 ± 1.00	2.35 ± 0.86	2.47 ± 0.92	-	-	-
Absolute	19.26 ± 5.19	0.59 ± 0.24	0.71 ± 0.34	< 0.001	< 0.001	0.812
SLF I						
Proportion	3.46 ± 0.93	0.71 ± 0.36	1.22 ± 0.44	< 0.001	0.001	0.225
Absolute	20.00 ± 5.85	0.17 ± 0.09	0.35 ± 0.15	< 0.001	< 0.001	0.142
SLF II						
Proportion	3.66 ± 1.17	1.12 ± 0.36	1.06 ± 0.55	< 0.001	< 0.001	0.986
Absolute	20.96 ± 6.09	0.27 ± 0.07	0.31 ± 0.18	< 0.001	< 0.001	0.902
SLF III						
Proportion	3.65 ± 1.08	1.33 ± 0.06	1.54 ± 1.02	< 0.001	0.060	0.816
Absolute	21.07 ± 6.40	0.33 ± 0.05	0.46 ± 0.33	< 0.001	< 0.001	0.695
IFOF						
Proportion	9.59 ± 1.22	3.80 ± 0.89	3.25 ± 0.94	< 0.001	< 0.001	0.656
Absolute	55.34 ± 8.73	0.95 ± 0.30	0.92 ± 0.33	< 0.001	< 0.001	0.989
AF						
Proportion	8.96 ± 1.38	1.58 ± 0.11	1.45 ± 0.13	< 0.001	< 0.001	0.044
Absolute	52.07 ± 10.88	0.39 ± 0.03	0.40 ± 0.05	< 0.001	< 0.001	0.832

Individual frontal association tracts (cingulum, uncinate fasciculus UF, frontal aslant tract FAT, superior longitudinal fasciculus SLF I, II and III, inferior fronto-occipital fasciculus IFOF, and arcuate fasciculus AF) in humans (n = 20), veverts (n = 4) and macaques (n = 5). Descriptive statistics and Games-Howell *post hoc* comparisons between species are given for proportional (normalized by total volume for each measure) and absolute volumes. See Results for Welch's ANOVA statistics.

Table 6. Proportional and absolute volume measurements of frontal association tracts in *in vivo* macaques

Tract	*In vivo* macaques	Comparison with *ex vivo* macaques			Comparison with *in vivo* humans		
		Welch's F	df within-groups	P	Welch's F	df within-groups	P
Cingulum							
Proportion (%)	3.65 ± 0.61	0.84	7.18	0.388	209.49	11.81	< 0.001
Absolute (ml)	1.57 ± 0.18	46.44	8.91	< 0.001	830.60	19.37	< 0.001
UF							
Proportion	3.09 ± 0.83	4.18	7.96	0.075	544.80	12.99	< 0.001
Absolute	1.34 ± 0.37	19.35	7.87	0.002	210.49	20.01	< 0.001
FAT							
Proportion	3.20 ± 0.48	2.83	6.21	0.142	1.38	14.36	0.259
Absolute	1.37 ± 0.12	16.86	4.83	0.010	237.00	19.07	< 0.001
SLF I							
Proportion	1.75 ± 0.74	1.14	7.68	0.318	33.75	5.26	0.002
Absolute	0.74 ± 0.24	10.54	8.60	0.011	215.52	19.21	< 0.001
SLF II							
Proportion	1.29 ± 0.61	0.01	7.95	0.921	44.42	9.30	< 0.001
Absolute	0.56 ± 0.28	3.36	8.55	0.102	222.56	19.26	< 0.001
SLF III							
Proportion	2.35 ± 0.36	1.34	4.42	0.306	17.23	22.79	< 0.001
Absolute	1.01 ± 0.16	11.92	5.50	0.016	196.12	19.08	< 0.001
IFOF							
Proportion	5.76 ± 1.60	8.34	6.08	0.027	19.73	4.98	0.007
Absolute	2.46 ± 0.55	32.61	8.37	< 0.001	724.84	19.49	< 0.001

Individual frontal association tracts (cingulum, uncinate fasciculus UF, frontal aslant tract FAT, superior longitudinal fasciculus SLF I, II and III and inferior fronto-occipital fasciculus IFOF) in *in vivo* macaques (n = 6). The arcuate fasciculus could not be reconstructed in *in vivo* macaques. Descriptive statistics and F, within-groups degrees of freedom (df) and P values are given. In all cases the between-groups df = 1. Welch's ANOVA was used to compare *in vivo* with *ex vivo* macaques, and *in vivo* with humans. Results are presented for proportional (normalized by total volume for each measure) and absolute volumes.